



ELSEVIER

Surface Science 380 (1997) 497–506

surface science

Submonolayer Au on Si(111) phase diagram

Richard Plass¹, Laurence D. Marks*

Department of Materials Science and Engineering, Northwestern University, Evanston, IL 60208-3108, USA

Received 1 August 1996; accepted for publication 26 December 1996

Abstract

Based on a review of the current literature, a surface phase diagram is proposed for the submonolayer Au on Si(111) system. Kinetic considerations are reviewed and key surface phase diagram features such as the $\theta < 0.4$ ML metastable Si(111)- $(\sqrt{3} \times \sqrt{3})R30^\circ$ -Au structure and the high temperature Si(111)- $(\sqrt{3} \times \sqrt{3})R30^\circ$ -Au to Si(111)-(1 \times 1)Au second order phase transition are discussed. Experiments to verify certain portions of the phase diagram are proposed. © 1997 Elsevier Science B.V.

Keywords: Adatoms; Compound formation; Diffusion and migration; Gold; Growth; Low index single crystal surfaces; Metal-semiconductor interfaces; Metal-semiconductor nonmagnetic thin film structures; Models of surface kinetics; Non-equilibrium thermodynamics and statistical mechanics; Semiconducting surfaces; Silicides; Silicon; Single crystal surfaces; Surface chemical reaction; Surface defects; Surface diffusion; Surface energy; Surface relaxation and reconstruction; Surface thermodynamics (including phase transitions)

1. Introduction

Though not as well studied as clean silicon surface reconstructions or the Ag on Si(111) system, the Au on Si(111) surface system displays a fascinatingly rich variety of structures and properties [1–39]. This, along with the potential use of gold as a surfactant for Si(111) homoepitaxy [10,12] make this system well worth understanding. Four different surface structures have been identified at various elevated temperatures and submonolayer gold coverages; “native” Si(111)-(7 \times 7) e.g. Ref. [40–43] (or simply 7 \times 7 hereafter),

Si(111)-(5 \times 2)Au e.g. Refs. [7–9,13–18] (or 5 \times 2 Au), Si(111)- $(\sqrt{3} \times \sqrt{3})R30^\circ$ e.g. Refs. [19–24] (or $\sqrt{3}$ Au), and Si(111)-(1 \times 1)Au [1,4,25] (or 1 \times 1 Au). Several studies of these structures have been done in situ [1–11], that is, the surface structure was observed at the same temperature at which it was formed. However, almost all of the data to date has been described in terms of “phase maps” (Fig. 1), i.e. diagrams showing under what conditions of temperature and composition the various phases appear. Similar to bulk materials, the proper description of the Au–Si surface system should be a phase diagram with temperature and coverage as the two axes and with phase boundaries based on thermodynamics principles.

In this note we will review the available information on this system, focusing primarily on the in situ data, and based upon this, propose a phase

*Corresponding author. Fax: +1 708 4917820;
e-mail: ldm@apollo.numis.nwu.edu

¹ Present address: Department of Physics, University of Wisconsin – Milwaukee, P.O. Box 413, Milwaukee, WI 53201, USA.

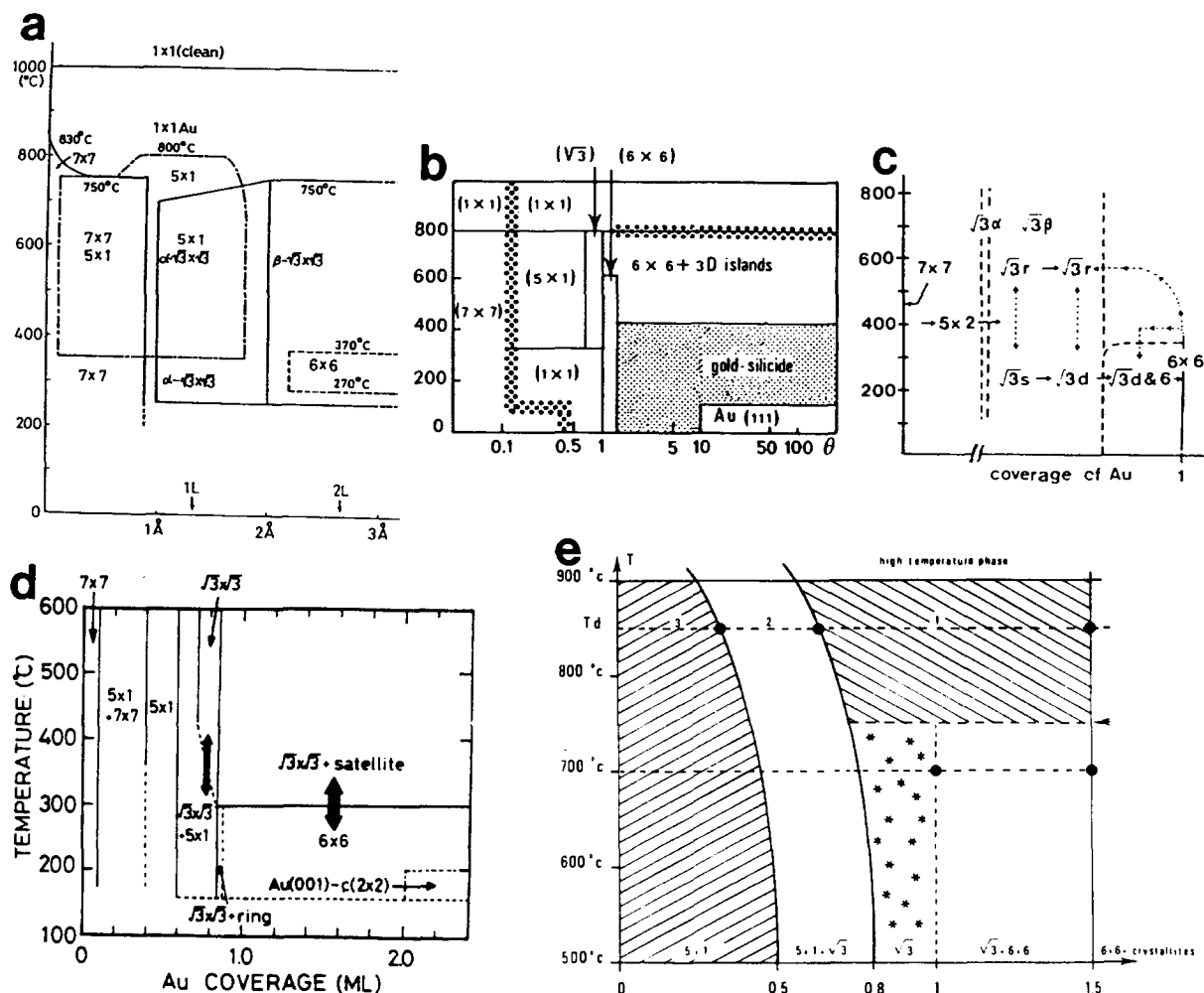


Fig. 1. Various surface phase maps that have been proposed for the Au on Si(111) system by: (a) Ino [34]; (b) Le Lay [28]; (c) Takahashi, Tanishiro and Takayanagi [5]; (d) Yuhara, Inoue and Morita [3]; (e) Le Lay, Manneville and Kern [25].

diagram up to one monolayer coverage. Identifying the phase transition locations of this diagram can lead to understanding and quantifying the various thermodynamic properties of the surface structures involved.

The structure of this note is as follows. First, we will briefly review the literature on submonolayer Au on Si(111) structures. In this section we will identify the gold coverages of the primary phases which anchor the deposition axis of the phase diagram. We will then use these anchors to interpret a number of in situ experiments, identifying both stable and metastable phases.

2. Submonolayer Au on Si(111) surface microstructures

Before discussing the Au on Si(111) surface phase diagram we will introduce the four phases present in the Au submonolayer regime. The nature of the 5×2 Au and $\sqrt{3}$ Au phases in particular needs to be addressed because there is considerable confusion (controversy) in the literature concerning their "saturation coverages" [17,26–30]. The concept of saturation coverage, in itself, is misleading since both 5×2 Au and $\sqrt{3}$ Au have the ability to vary their gold content and should be considered

“surface solutions”. Thermodynamics then dictates that the gold coverage *range* over which they cover the surface must vary with temperature. The exact annealing and temperature measurement conditions vary from one study to another, in part explaining the debate. However, the variations in reported saturation coverages are very large. For instance, the reported saturation coverages for 5×2 Au range from 0.40 ML e.g. Refs. [15,28] to 0.78 ML [29], and for $\sqrt{3}$ Au from 0.66 ML [26,30] to 1.17 ML [29]. Given these discrepancies it is important to find an “anchor” coverage for each of these structures.

Besides gold coverage, another useful parameter for comparing different Au–Si surface structures is the silicon surface density, defined as the number of surface silicon atoms per 1×1 unit cell e.g. Ref. [41,42]. The average silicon surface densities of the four structures are included in the following discussions and we will treat this parameter as the gold coverage’s complement in the same way binary bulk phase diagrams have complementing composition axes.

2.1. *Si(111)-(7 × 7)*

The dimer adatom stacking fault (DAS) atomic structure of 7×7 (Fig. 2a) has been well studied [40–43 and references therein], both before and after its atomic structure was solved by Takayanagi and coworkers in 1985 [40]. It is sufficient to note here that this is a complex structure, and that there is no simple gold substitutional site in this structure – the lowest gold saturation coverage structure, 5×2 Au, nucleates at 7×7 domain boundaries [5–9,13,14]. The relevance of a stable gold substitutional site will become clear later. The 7×7 silicon surface density is 2.08.

2.2. *Si(111)-(5 × 2)Au*

The atomic structure of 5×2 Au is not yet fully accepted in the literature, but a consensus seems to be growing [9,15,31] that the structure consists of two rows of gold atoms along with some type of silicon structure (gold coverage, 0.40 ML). Our proposed atomic structure is shown in Fig. 2b. (The only difference in this model from the one

reported earlier [15] is that a set of Si atoms are in the same plane forming a chained π bond. The most likely bonding configuration, of a possible three, is shown.) HREM results [15] conclusively identify four gold atom sites per 5×2 unit cell forming two gold rows. Not yet clear is whether there is a fifth, partially occupied gold site which may appear as protrusions in STM images [7–9,13,14,16,29,32]. If the protrusions are gold atoms, the occupancy of the fifth site would be on the order of 0.03 ML bringing the “saturation coverage” of 5×2 Au to about 0.43 ML with a lower bound of 0.40 ML. Several STM studies have found that the density of the protrusions remains constant with coverage [7–9,16,29], which implies that they are silicon. However one study [13] (in which the domains were longer) found that the protrusion density tracked with gold coverage, implying that the gold coverage could vary from 0.40 to 0.45 ML. This is the range over which 5×2 Au is a “surface solution” with variable gold content. The protrusions, assuming they are gold atoms, are illustrated as the larger, dark atoms in the 5×2 Au model in Fig. 2b.

While the differences in protrusion surface density seen (or not seen) by various groups will be discussed below, for now we assume the value of 0.275 to 0.32 gold atoms per unit cell [16,29] (or 0.0275 to 0.032 ML of gold) for a total 5×2 Au “saturation” coverage of about 0.43 ML. (While the issue of whether 5×2 Au is a line compound in gold coverage or a limited surface solution remains to be solved by further experiments, it does not change the primary features of the surface phase diagram.)

Finding reliable 5×2 Au saturation coverages is important because while most of the in situ and annealed surface studies have their own coverage calibration, the pivotal LEEM study of Świąch, Bauer and Mundschau [1] does not. Instead it reports precise values of the saturation coverage ratios. Since this study provides many key pieces of in situ information, a reliable coverage standard must be determined. The LEEM study used an assumed $\sqrt{3}$ Au coverage of 0.66 ML; a recent study [29] reformulated the conclusions based on a 1.17 ML $\sqrt{3}$ Au saturation coverage. A value of 1.17 ML for $\sqrt{3}$ Au and the LEEM based ratios

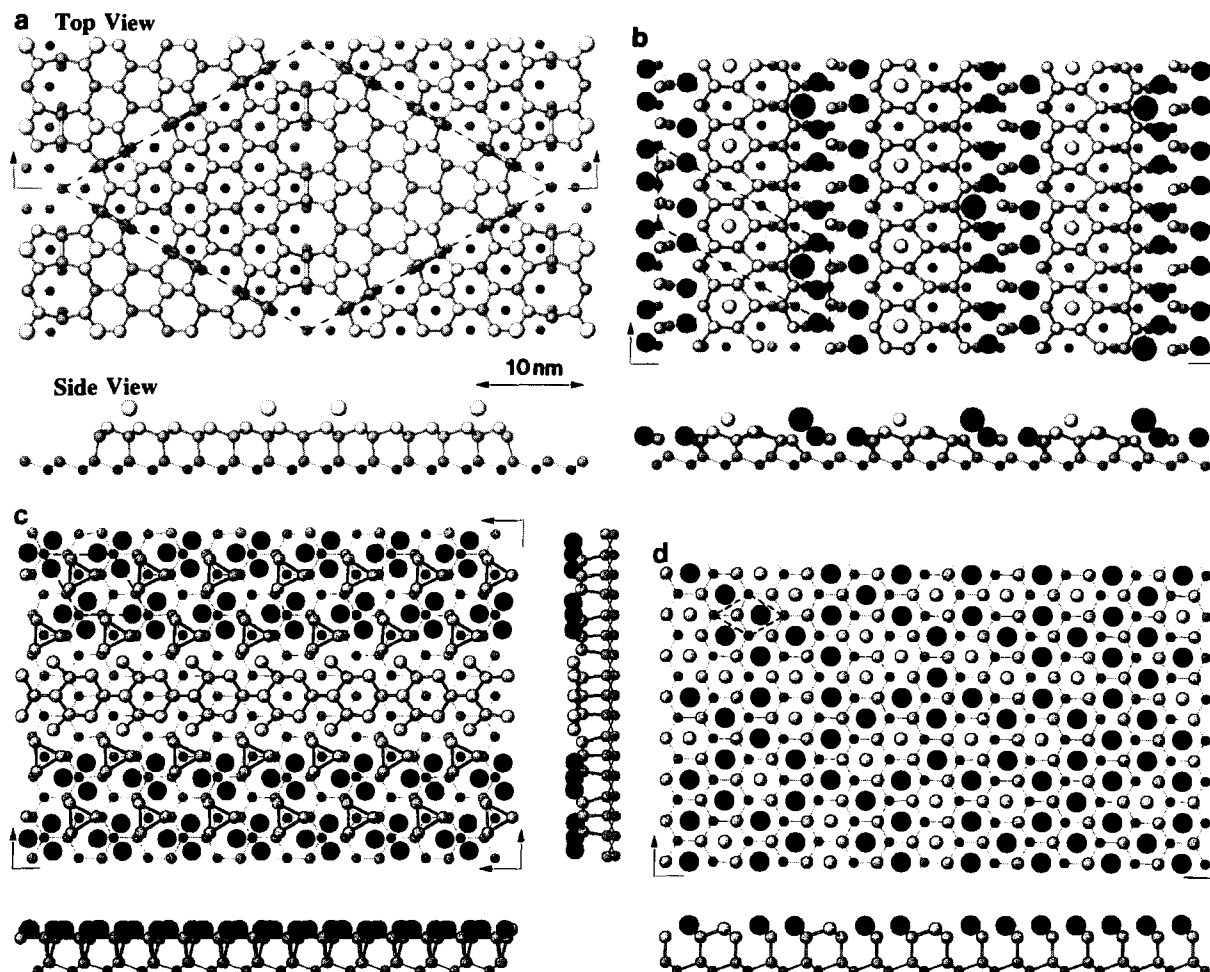


Fig. 2. Top and side view schematics of proposed models for (a) Si(111)-(7×7) [40,43], (b) Si(111)-(5×2)Au [15] with gold protrusions, (c) Si(111)-(√3×√3)R30°-Au [19] with a vacancy type domain wall and (d) Si(111)-(1×1)Au. Large dark balls represent gold atoms while smaller lighter atoms are silicon. Primitive unit cells are indicated with lines, the vertical positions of atoms are arbitrary.

give 0.78 ML for the coverage of 5×2 Au, which contradicts the HREM and STM data; the original formulation may not be far off. In the present study all LEEM coverage results are calculated based on the a 5×2 Au saturation coverage of 0.43 ML. 5×2 Au's reported silicon surface densities range from 1.3 [9] to 1.6 [18], the structure in Fig. 2b has a density of 1.5 [15].

2.3. Si(111)-(√3×√3)R30°-Au

The majority of the literature agrees that this surface is either one of two types of missing top

layer (MTL) structures, either the conjugate honeycomb chained trimer model [21] or the missing top later twisted trimer model [24] (Fig. 2c). The slight differences between these are irrelevant here, but the fact that the saturation coverage of either model is 1.0 ML is important. Ion scattering results from √3 Au that has been annealed for long periods [2,3,24] have found the “stable” (in the prolonged anneal, “thermodynamic” sense) saturation coverage of this structure is 0.85 ML. STM studies [26,30] reveal that below this coverage the average √3 Au domain size is 50 Å. This suggests that the √3 Au domain walls are gold deficient. A

proposed [19] vacancy type domain wall structure is also shown in Fig. 2c. For coverages above 0.85 ML Nogami et al. and Takami et al. found that the average domain size shrink linearly with increasing coverage. At present it is not clear what this change in surface morphology is due to [22,33]. Ideally an MTL structure has a silicon surface density of 1.0 but the presence of silicon filled vacancy domain walls would bring this value up to about 1.13 based on 50 Å sized domains [26].

2.4. *Si(111)-(1 × 1)-Au*

Not much is known about this high temperature phase except that it displays a 1×1 LEED pattern [1,5,6,25] and contains sufficient gold that upon cooling the 5×2 Au and/or $\sqrt{3}$ Au structures form. It should be noted that in the elevated temperature range in which this phase appears substantial gold diffusion into the bulk [2,3] as well as some gold desorption [25] may occur. As we will see later, the most likely atomic structure for this phase is gold randomly substituted into a surface silicon double layer. Befitting its liquid like character, 1×1 Au's gold coverage and silicon surface density can vary drastically.

3. Phase diagrams

3.1. Stable phases from in situ studies

Fig. 3 shows the phases found in in situ studies to date as functions of the temperature and gold coverage/silicon surface density. The set of dashed curves represent potential phase boundaries. These have not been derived from any energy parameters but with more experiments they could be used to derive the key energy parameters, as will be discussed later. The phase diagram is complex, with lower coverage eutectoid and higher coverage peritectoid regions, assuming the high temperature 1×1 Au and the $\sqrt{3}$ Au phases are related by a second order phase transition.

Among the data points shown in Fig. 3 there are a handful that are pivotal. The first are the LEEM results of Świąch and coworkers [1] and the RHEED results of Diamon et al. [4], below, at, and above the saturation coverage of 5×2 Au

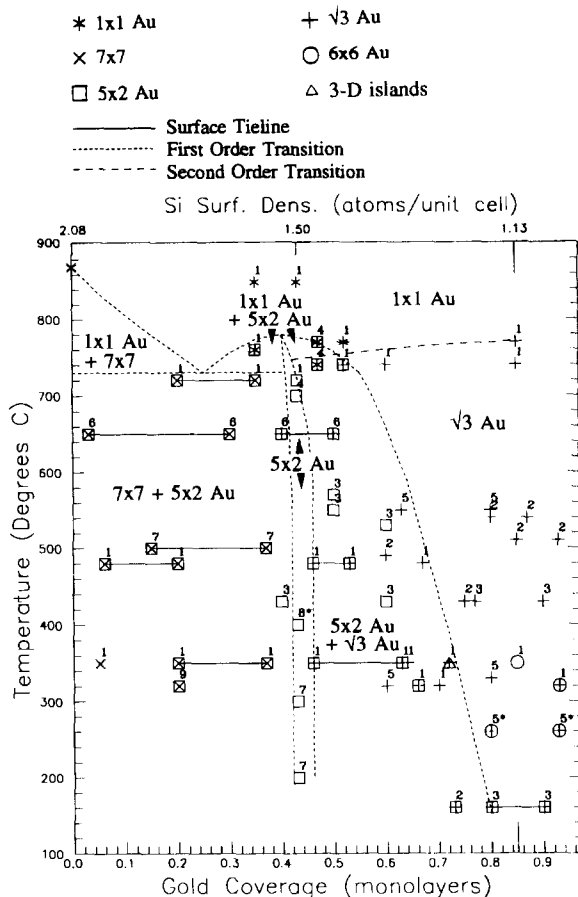


Fig. 3. Proposed submonolayer Au on Si(111) surface phase diagram with literature in situ experimental results shown. The number over the symbol corresponds to its reference number, except (for clarity) 7 corresponds to [7–9], 8 to [10] and 9 to [11]. Single symbols represent a reported surface completely covered by that symbol's surface structure. Overlapping symbols represent coexistence of the corresponding structures on the surface. For example a square with an "x" on it means 7×7 and 5×2 Au are both present on the surface. Solid lines represent experimental tielines between surfaces with mixed compositions. The short dashed curves are potential locations of first order phase transitions between different phase regions. The longer dash curve represent a second order transition. All data points (except the RBS studies; 2 and 3) have an expected error of at least ± 0.05 ML based on crystal monitor/AES limitations and a temperature error of at least $\pm 10^\circ\text{C}$ based on typical pyrometer limitations. Data points were taken either directly from the text of references or from coverage estimates based on the reference's images. Starred (*) reference numbers indicate the coverage was estimated.

for temperatures above 700°C. These results define parts of the 1×1 Au to 1×1 Au + 5×2 Au and the 1×1 Au + 5×2 Au to 7×7 + 5×2 Au phase boundaries. The LEEM results are particularly interesting in that they show anisotropic 5×2 Au growth and decay during the reversible 1×1 Au to 5×2 Au transition.

Below the eutectoid/peritectoid temperature (around 730°C, in agreement with Ino's surface phase map [34], Fig. 1a) several studies have shown that 5×2 Au nucleates at surface steps and 7×7 domain walls [1,5–9]. As the tielines in this region show, 5×2 Au domains grow, consuming all the available gold. (The LEEM results for low gold coverages at 350°C should be used with some reservation since the domain size is close to the LEEM resolution.) Above the eutectoid/peritectoid temperature it is clear from LEEM that 5×2 Au and 1×1 Au coexist. This means that at some lower gold coverage (arbitrarily shown at 0.25 ML) there must be a eutectic point between 5×2 Au + 1×1 Au, pure 1×1 Au, and 1×1 Au + 7×7 . The 7×7 region may or may not have adsorbed gold in it. Although there is no experimental evidence to support this eutectic point, it is also seen in Ino's surface phase map (Fig. 1a) and implies that the "melting point" of 5×2 Au, and therefore 5×2 Au's cohesive energy, is close to that of 7×7 .

The scatter of data points for the pure 5×2 Au phase is rather large for the in situ studies. Hence the coverages for the 5×2 Au are based on the structural data discussed previously, taking the protrusions to be gold sites. The results of Świąch and coworkers [1] and Diamon and coworkers [4] set the temperature limits. The boundaries of the pure 5×2 Au phase curve and approach each other as they near the eutectoid/peritectoid temperature, indicating that the gold protrusions become less stable (compared to the $\sqrt{3}$ Au trimer site) with increasing temperature. This implies that 5×2 Au is not a line compound even though it acts like one over most of the temperature range. (A line compound interpretation for 5×2 Au, i.e. a straight vertical line near 0.43 ML, would also match the experimental data, given their scatter.) The curving of these boundaries toward lower coverage can explain why the 5×2 Au/ $\sqrt{3}$ Au coverage ratio, carefully measured by Świąch and coworkers [1],

remains constant over a large temperature range while one set of STM results [13] show the 5×2 Au saturation coverage decreases with increasing temperature.

The constant (with respect to temperature) 5×2 Au to $\sqrt{3}$ Au coverage ratio provides a definite link between the phase boundaries that limit the 5×2 Au + $\sqrt{3}$ Au coexistence region. The 5×2 Au + $\sqrt{3}$ Au tielines, particularly the result of Yuhara and coworkers [2,3] at 0.75 ML and 150°C, as well as the 5×2 Au + $\sqrt{3}$ Au to 1×1 Au + $\sqrt{3}$ Au transition seen by LEEM at about 750°C, define the rest of the "liquidus" phase boundary which curves strongly toward lower coverages with increasing temperature. This is in agreement with the surface phase maps of Le Lay and Yuhara [3,25] (Figs. 1d and 1e).

The final key feature of the surface phase diagram is a second order phase transition seen between $\sqrt{3}$ Au and 1×1 Au. The high temperature (1050°C) profile images of Kamino et al. [35] show a surface layer with much stronger contrast than the bulk and which has about the correct height for a missing top layer structure. Thus a reasonable model for the "liquid" 1×1 Au surface is gold in a missing top layer type configuration but where thermal vibrations inhibit the formation of gold trimers. If the gold coverage is less than one monolayer, silicon double layer units must also be present to maintain layer continuity. Otherwise the desorption energy of Au [25] would be significantly lower. Essentially, gold substitutes randomly into an ideal bulk terminated Si(111) surface and stabilizes it, much as excess silicon apparently does in clean, high temperature Si(111)-(1 \times 1) e.g. Refs. [41,42]. As the temperature drops to about 750°C strong Au–Au and Si–Si bonding leads to trimerization and hence the $\sqrt{3}$ Au structure as indicated by the almost horizontal long dashed curve in Fig. 3.

Based on this second order transition argument, one would expect that in the range 600 to 750°C the average Au trimer spacing will vary linearly from about 2.70 to 3.84 Å, respectively. A similar effect is seen in the Pb on Ge(111) system [44]. RHEED studies [36] indirectly support this, since the average $\sqrt{3}$ Au domain size increases with temperature. More definitive evidence for a second order phase transition is the LEEM study where

at temperatures above 700°C it was impossible to distinguish regions of 1×1 Au from $\sqrt{3}$ Au despite the presence of weak $\sqrt{3} \times \sqrt{3}$ diffraction spots. The near 3.84 Å Au to Au spacing in the 5×2 Au structure also circumstantially supports this proposed second order transition.

3.2. Metastable structures

Fig. 4a is a magnification of Fig. 3 which also shows two metastable gold induced surface recon-

structions, one strongly backed by experiment, the other not. The presence of both structures relies on slow kinetics due to either: (1) A high activation barrier to removal of silicon from the 7×7 structure and/or nucleation of 5×2 Au. (2) Slow silicon surface diffusion. As will be seen, evidence supports the latter factor.

The most clearly backed structure is metastable $\sqrt{3}$ Au at coverages below 0.4 ML. The phase diagram at higher temperatures excludes the coexistence of 7×7 and $\sqrt{3}$ Au; therefore it is initially

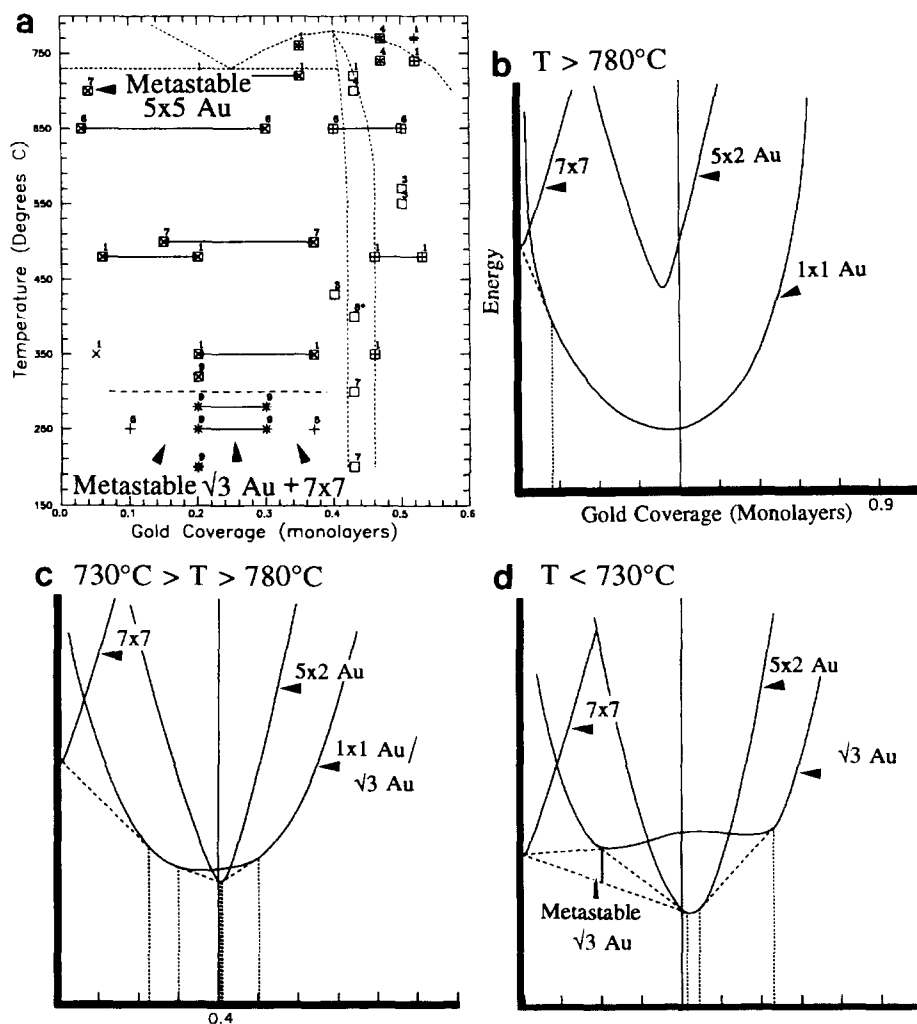


Fig. 4. (a) Magnification of the Au on Si(111) surface phase diagram including metastable surface structures. The number above a data point again corresponds to its reference number. (b–d) Schematic free energy curves which illustrate how the real free energy curves interact to generate the low coverage Au on Si(111) phase diagram features, in (b) the 780 to 870°C, (c) the 730 to 780°C and (d) the below 730°C temperature ranges.

surprising to see them coexist at lower temperatures. The work of Tanishiro and Takayanagi [6] and especially of Shibata, Kimura and Takayanagi [11], for the metastable $\sqrt{3}$ Au structure between 0.2–0.4 ML and 200–280°C, is significant in that they also determined that it forms by an island–hole pair mechanism [11]. The similarity in the irreversible transition temperature from 2×1 to 5×5 (350°C) [45] and from low coverage $\sqrt{3}$ Au to 5×2 Au (300°C) is also striking. As Shibata and coworkers point out in proposing the hole–island mechanism, much less silicon transport is required to form the $\sqrt{3}$ Au structure than to form 5×2 Au. The same “sluggish” silicon kinetics that drives the formation of 2×1 upon cleavage rather than the more stable 5×5 and 7×7 is likely also at work in the formation of $\sqrt{3}$ Au rather than 5×2 Au at these temperatures. (The metastable 2×1 structure arises because formation of the 7×7 structure requires substantial silicon displacements [37,45]). The schematic free energy curves of the major temperature regimes (shown in Figs. 4b–d) illustrate how the metastable $\sqrt{3}$ Au free energy gap might arise. (These schematic free energy curves also predict that the 5×2 Au “surface solution” is more ideal, in a thermodynamic sense, than the $\sqrt{3}$ Au/ 1×1 Au “surface solution” as is manifest by the “hump” in the phase diagram below 0.43 ML and 780°C.)

The presence of metastable $\sqrt{3}$ Au in the phase diagram leads to an important conclusion. In the case of the quenched Si(111)-(1 \times 1) surface [41,42], which local silicon structure forms depends more on the concentration of the mobile (Si) species present at the formation site than stress requirements of the surface. In the case of submonolayer gold, if mobile silicon is available the 5×2 Au surface grows from defect sites. If the surface is “mobile silicon starved”, the $\sqrt{3}$ Au structure forms.

The other metastable structure is backed solely on STM observation of an annealed 5×5 protrusion pattern on terraces at 700°C [8]. The theoretical coverage of these protrusions, 0.04 ML assuming they are gold, gives the saturation coverage. Since not many unit cells of this surface were shown and studies have not confirmed this result, it may be a poorly ordered version of 5×2 Au.

4. Kinetics

Given the somewhat better understanding of the submonolayer Au on Si(111) surface phase diagram that the above discussion gives us, the next logical course of action is to determine relevant thermodynamic parameters of the various structures which allow us to reasonably match the proposed phase boundaries indicated in Fig. 2. Experimentally determined activation energies for Au desorption and bulk diffusion set limits on the values of the surface thermodynamic parameters. Le Lay, Manneville and Kern [25] determined Au desorption activation energies of gold from greater than one monolayer coverage structures is 3.3 eV per Au atom while for gold desorption from $\sqrt{3}$ Au it is 3.6 eV and from 5×2 Au it is 3.7 eV. These results are striking considering that Au sublimation from bulk Au requires 3.67 eV at 850°C [25]. Le Lay and coworkers determined that gold loss to desorption was only significant for temperatures over 800°C with surface gold “half lives” on the order of minutes. Gold can also be lost from the surface through diffusion into the bulk, here again we see a jump in activation energy in going below one monolayer. Between 700 and 1200°C Struthers [37] found the bulk silicon diffusion activation energy for high Au coverages is 1.1 eV which agrees well with the value of Yuhara et al. [3]; 1.3 eV obtained between 430 and 490°C. Below one monolayer Yuhara found the activation energy for gold diffusing from the $\sqrt{3}$ Au surface structure into the bulk is 2.5 ± 0.5 eV and from 5×2 Au it is 2.8 ± 1.7 eV (between 500 and 580°C). The third “sink” for gold atoms is island nucleation and while no experimental activation energies have been obtained for this process we can expect it to be larger than (but roughly the same order of magnitude as) the value in the Ag on Si(111) system; 0.05 ± 0.03 eV [47]. This, in conjunction with slow surface diffusion, sets the lower temperature limit for the formation of submonolayer structures at 100–150°C since below this temperature gold will likely nucleate into islands given sufficient time (centuries).

An underlying assumption in any thermodynamic treatment is that the system is “closed” with respect to the mass of the constituents, the amounts

of reactants stay constant over the temperature range of interest. Normally this condition is not easily satisfied for metal on semiconductor systems since metal desorption, diffusion into the bulk and nucleation all act as “sinks” for the metal. Metal addition to compensate for these effects and thus establish a “steady state” constant surface metal content is quite difficult. However, we can see in the supermonolayer to submonolayer jump in the activation energies of desorption and bulk diffusion that, within a certain temperature (100–900°C), time (tens of minutes) and coverage (below 1 ML) “window”, the approximation of constant gold coverage is reasonable.

While these activation energies establish that thermodynamic treatment is possible in the window, another requirement is that gold and silicon can readily move between different surface structures in the window and thus establish equilibrium amounts of surface area among the different surface structures. This means some gold and silicon atoms must have sufficient energy to allow them to diffuse over the different surface structures.

Gold on Si(111) electromigration studies [38] have found activation energies for Au adatom migration over Au over $\sqrt{3}$ Au to be 1.3 eV, for Au over 5×2 Au, Lifshits and coworkers found 1.6 eV while Yasunaga and Sasuga [39] found 0.77 eV. For Au over 7×7 , Lifshits and coworkers found an activation energy of 2.0 eV while Yasunaga and Sasuga found 1.2 eV, these electromigration studies were conducted in the 500 to 900°C temperature range. From RBS studies Yuhara et al. found, in the 500 to 580°C temperature range, an activation energy in Au atoms moving from the $\sqrt{3}$ Au to the 5×2 Au structures of 1.6 ± 0.9 eV [2,3]. Thus we see that some Au atoms will have sufficient energy to move between the different structures in the window since these surface diffusion activation energies are substantially lower than those of desorption or bulk diffusion.

5. Discussion

In reviewing the relevant literature on the submonolayer Au on Si(111) system this note has intended to set the groundwork for more focused and detailed work on this system’s phase diagram.

As a result several key points can be may and several areas of needed future work have been identified.

The literature strongly supports the following conclusions. (1) Gold does not appear to find a stable substitutional site in 7×7 . (2) Both the 5×2 Au and especially the $\sqrt{3}$ Au structures appear to be able to vary their gold content to a (limited) degree which varies strongly with temperature. (3) $\sqrt{3}$ Au appears to undergo a second order transition to the 1×1 Au phase somewhere above 600°C. (4) The presence of a low coverage, metastable $\sqrt{3}$ Au phase sheds significant light on the surface diffusion kinetics of the system.

Further work is needed to confirm predicted features of the surface phase diagram, namely: (1) coexistence of a mixed 1×1 Au and 7×7 surface at very low coverages and elevated temperature. (2) Elevated temperature diffraction studies to confirm the nature of the second order $\sqrt{3}$ Au to 1×1 Au phase transition by measuring the average $\sqrt{3}$ Au trimer spacing with temperature. (3) A theoretical simulation of the energetics of the system to determine the thermodynamic parameters which correspond to the system’s apparent phase boundaries.

Some final points can be made concerning the relationship between surface bonding of Au and Si, and the bulk. The bulk phase diagram is a “deep” eutectic, with a eutectic temperature of 363°C; except for an amorphous phase from rapid quenching and some poorly defined, metastable silicides e.g. Refs. [48,49], no other phases are known. From the thermodynamic analysis of Cros and Muret [50] the deep eutectic is due to a high entropy of mixing of Si and Au in the liquid phase. All the surface phases below one monolayer are stable above the eutectic temperature, implying some type of surface stabilized Au–Si bond. But as the coordination around the Au becomes bulk-like, Au–Au and Si–Si bonds form rather than surface compounds. Interestingly, the gold containing surface phases appear to contain only Au to bulk Si bonds, no Au–Si–Au bonds, which is in line with the bulk Au–Si behavior. Why the surface Au–Si bond is so anomalously strong is unclear, although we have suggested [19,33] that the bonding may be more related to surface stress relief than genuine chemical bonding. More work, partic-

ularly theoretical calculations, may clarify this issue.

Acknowledgements

We would gratefully like to acknowledge T. Hasegawa, A. Ichimiya, T. Kamino, J. Nogami, J.D. O'Mahony, H. Saka, L. Seehofer, K. Yagi and J. Yuhara for their valuable correspondences and/or providing preprints of their work. This research was supported by the Air Force Office of Scientific Research under Grant #F49620-92-J-0250.

References

- [1] W. Świąch, E. Bauer and M. Munschau, *Surf. Sci.* 253 (1991) 283.
- [2] J. Yuhara, M. Inoue and K. Morita, *J. Vac. Sci. Technol. A* 10 (1992) 334.
- [3] J. Yuhara, M. Inoue and K. Morita, *J. Vac. Sci. Technol. A* 10 (1992) 3486.
- [4] H. Diamon, C. Chung, S. Ino and Y. Watanabe, *Surf. Sci.* 235 (1990) 142.
- [5] S. Takahashi, Y. Tanishiro and K. Takayanagi, *Surf. Sci.* 242 (1991) 73.
- [6] Y. Tanishiro and K. Takayanagi, *Ultramicroscopy* 31 (1989) 20.
- [7] T. Hasegawa, K. Takata, S. Hosaka and S. Hosoki, *J. Vac. Sci. Technol. B* 9 (1991) 758.
- [8] T. Hasegawa, S. Hosaka and S. Hosoki, *Jpn. J. Appl. Phys.* 31 (1992) L1492.
- [9] T. Hasegawa, S. Hosaka and S. Hosoki, *Surf. Sci.* 357 (1996) 858.
- [10] H. Minoda, Y. Tanishiro, N. Yamamoto and K. Yagi, *Appl. Surf. Sci.* 60 (1992) 107.
- [11] A. Shibata, Y. Kimura and K. Takayanagi, *Surf. Sci.* 273 (1992) L430.
- [12] G.D. Wilk, R.E. Martinez, J.F. Chervinsky, F. Spaepen and J.A. Golovchenko, *Appl. Phys. Lett.* 65 (1994) 866.
- [13] J.D. O'Mahony, J.F. McGilp, C.F.J. Flipse, P. Weightman and F.M. Leibsle, *Phys. Rev. B* 49 (1994) 2527.
- [14] J.D. O'Mahony, C.H. Patterson, J.F. McGilp, F.M. Leibsle, P. Weightman and C.F.J. Flipse, *Surf. Sci.* 277 (1992) L57.
- [15] L.D. Marks and R. Plass, *Phys. Rev. Lett.* 75 (1995) 2172.
- [16] A.A. Baskii, J. Nogami and C.F. Quate, *Phys. Rev. B* 41 (1990) 10247.
- [17] Ch. Schamper, W. Moritz, H. Schluz, R. Feidenhans'l, M. Nielsen, F. Grey and R.L. Johnson, *Phys. Rev. B* 43 (1991) 12130.
- [18] L.E. Berman, B.W. Batterman and J.M. Blakely, *Phys. Rev. B* 38 (1988) 5397.
- [19] R. Plass and L.D. Marks, *Surf. Sci.* 342 (1995) 233.
- [20] J. Quinn, F. Jona and P.M. Marcus, *Phys. Rev. B* 46 (1992) 7288.
- [21] Y.G. Ding, C.T. Chan and K.M. Ho, *Surf. Sci.* 275 (1992) L691.
- [22] J. Falta, A. Hille, D. Novikov, G. Materlik, L. Seehofer, G. Falkenberg and R.L. Johnson, *Surf. Sci.* 330 (1995) L673.
- [23] Y. Kuwahara, S. Nakatani, M. Takahasi, M. Aono and T. Takahashi, *Surf. Sci.* 310 (1994) 226.
- [24] M. Chester and T. Gustafsson, *Surf. Sci.* 256 (1991) 135.
- [25] G. Le Lay, M. Manneville and R. Kern, *Surf. Sci.* 65 (1977) 261.
- [26] J. Nogami, A.A. Baski and C.F. Quate, *Phys. Rev. Lett.* 65 (1990) 1611.
- [27] K. Higashiyama, S. Kono and T. Sagawa, *Jpn. J. Appl. Phys.* 25 (1986) L117.
- [28] G. Le Lay, *J. Cryst. Growth* 54 (1981) 551; *Surf. Sci.* 132 (1983) 169.
- [29] L. Seehofer, S. Huhs, G. Falkenberg and R.L. Johnson, *Surf. Sci.* 329 (1995) 157.
- [30] T. Takami, D. Fukushi, T. Nakayama, M. Uda and M. Aono, *Jpn. J. Appl. Phys.* 33 (1994) 3688.
- [31] Y. Yabuuchi, F. Shoji, K. Oura and T. Hanawa, *Surf. Sci.* 131 (1983) L412.
- [32] Y. Yagi, K. Kakitani and A. Yoshimori, private communication (October 1995).
- [33] R. Plass, L.D. Marks and D.L. Dorset, in preparation.
- [34] S. Ino, *Reflection High-Energy Electron Diffraction and Reflection Electron Imaging of Surfaces*, Eds. P.K. Larson and P.J. Dobson (Plenum, New York, 1988).
- [35] T. Kamino, T. Yaguchi, M. Tomita and H. Saka, *Phil. Mag.* to be published.
- [36] S. Hasegawa and S. Ino, *Int. J. Mod. Phys. B* 7 (1993) 3817.
- [37] J.D. Struthers, *J. Appl. Phys.* 27 (1956) 1560.
- [38] V.G. Lifshits, V.B. Akilov, B.K. Churusov and Yu.L. Gavriljuk, *Surf. Sci.* 222 (1989) 21.
- [39] H. Yasunaga and E. Sasuga, *Surf. Sci.* 231 (1990) 263.
- [40] K. Takayanagi, Y. Tanishiro, S. Takahashi and M. Takahashi, *Surf. Sci.* 164 (1985) 367.
- [41] Y.N. Yang and E.D. Williams, *Phys. Rev. Lett.* 72 (1994) 1862.
- [42] Y.N. Yang and E.D. Williams, *Scanning Microscopy* 8 (1994) 781.
- [43] R.D. Twesten and J.M. Gibson, *Ultramicroscopy* 53 (1995) 223.
- [44] G.E. Franklin, M.J. Bedzyk, J.C. Woicik, C. Liu, J.R. Patel and J.A. Golovchenko, *Phys. Rev. B* 51 (1996) 2440.
- [45] R.M. Feenstra and M.A. Lutz, *Phys. Rev. B* 42 (1990) 5391; *Surf. Sci.* 243 (1991) 151.
- [46] K. Miki, Y. Morita, H. Tokumoto, T. Sato, M. Iwatsuki, M. Suzuki and T. Fukuda, *Ultramicroscopy* 42 (1992) 851.
- [47] G. Raynerd, T.N. Doust and J.A. Venables, *Surf. Sci.* 261 (1992) 251.
- [48] G.A. Andersen, J.L. Bestel, A.A. Johnson and B. Post, *Mat. Sci. and Eng.* 7 (1971) 77.
- [49] B.Y. Tsaur and J.W. Mayer, *Phil. Mag.* A 43 (1981) 345.
- [50] A. Cros and P. Muret, *Mat. Sci. Rep.* 8 (1992) 271.